πp elastic scattering from 67 to 139 MeV

J. T. Brack, J. J. Kraushaar, J. H. Mitchell, R. J. Peterson,
R. A. Ristinen, and J. L. Ullmann
Department of Physics, University of Colorado, Boulder, Colorado 80309

D. R. Gill, R. R. Johnson, D. Ottewell, F. M. Rozon, M. E. Sevior, G. R. Smith,
F. Tervisidis, and R. P. Trelle
University of British Columbia and TRIUMF, Vancouver, British Columbia, Canada V6T 2A3

E. L. Mathie
University of Regina, Regina, Saskatchewan, Canada S4S 0A2
(Received 21 July 1986)

Measurements of $\pi^{\pm}$p elastic differential cross sections have been made at seven incident pion energies from 66.8 to 138.8 MeV. These measurements have statistical accuracy of 1.5—3.3 % for π^+ and 2.7—19.0 % for π^-. The absolute normalization uncertainties are 1.2—2.5 % for π^+ and 1.2—3.2 % for π^-. Extensive tests were made to ensure that systematic errors were properly evaluated.

I. INTRODUCTION

Determination of the correct phase shifts for pion-nucleon scattering is essential for understanding the results of a wide variety of pion-nucleus experiments as well as for understanding the basic pion-nucleon interaction itself. While a determined effort has been made in recent years to provide the necessary πN cross sections (total cross sections, differential cross sections, and polarization data), there still appear to be major discrepancies in the low energy πp elastic scattering data published by different research groups.

Within the past 20 years πp elastic scattering measurements have been reported by four research groups[1–4] for positive pions, and two research groups[1,4] for negative pions in the energy region 60—143 MeV. Two sets of the π^+ measurements[3,4] were made at LAMPF, as was one set of the π^- measurements.[4] The other groups worked at CERN (Ref. 1) and at Saclay.[2] All of these efforts utilized a liquid hydrogen target but the counter techniques employed were quite different from group to group.

The π^+p measurements of Bussey *et al.*[1] include data at 94.5, 114.1, 124.8, and 142.9 MeV as well as extensive data at several higher energies. Bertin *et al.*[2] have furnished π^+p elastic cross sections at seven energies between 20.8 and 95.9 MeV, and Ritchie *et al.*[3] have published π^+p data at seven energies between 65 and 140 MeV. The most recent π^+p data are those of Frank *et al.*[4] at four energies from 30 to 90 MeV.

There have been considerably fewer π^-p than π^+p elastic scattering measurements because of the lower intensity of available π^- beams. Prior to 1983, the only modern published π^-p elastic cross sections in this energy region were those of Bussey *et al.*[1] at 88.5, 119.3, and 144.1 MeV, which are part of a data set extending over eight energies from 88.5 to 291.5 MeV. In addition, there now are the recent π^-p data of Frank *et al.*[4] in the energy range 30—90 MeV.

The recent work of Frank *et al.*[4] was undertaken to remedy the lack of π^-p elastic scattering data and to improve on existing π^+p measurements in this energy region. They determined the $\pi^{\pm}$p cross sections at 30, 50, 70, and 90 MeV over the angular range 50°—105° with relatively small statistical ($\approx$4%) and systematic ($\approx$2%) uncertainties, but with absolute normalization uncertainties as large as 20% for some of their data sets. Unfortunately, there are relatively large discrepancies between the cross sections of Frank *et al.*[4] and many of the earlier $\pi^{\pm}$p results. For example, the π^+p cross sections of Bussey *et al.*[1] are 20% larger than those of Frank *et al.*[4] at some pion energies and scattering angles. There are also discrepancies that range from 15% to 25% at large angles between the π^+p results of Bertin *et al.*[2] and those of Ritchie *et al.*[3] at 65 and 80 MeV where the quoted uncertainties of both groups are typically 3%.

Furthermore, the work of Frank *et al.*[4] is the most modern and comprehensive in scope and yet their reported cross sections differ markedly at some angles and energies from phase-shift predictions based on a large body of previous pion scattering and charge-exchange data. This problem has been addressed by Sadler[5] and by Siegel and Gibbs,[6] but there is no apparent resolution to the large discrepancies in the published data. This poses a major problem for the intermediate energy nuclear physics community that relies on phase-shift analyses of low-energy pion-nucleon and pion-nucleus reaction data, both for normalization and for reaction calculations.

The present experiment is an attempt to provide a reliable data set for both π^+p and π^-p elastic scattering by using an absolutely calibrated apparatus. The target was solid (CH_2), of directly measurable thickness and hydrogen content. Each incident pion was counted, and counter dimensions and efficiencies were accurately measured. All necessary systematic corrections due to pion decay,

multiple scattering, etc. can be easily assessed by variations in the geometry of the experiment to diminish errors and enable understanding of the systematic uncertainties.

II. EXPERIMENTAL PROCEDURE

The experiment was carried out on the $M11$ pion channel at TRIUMF with the use of five pion scintillation counter telescopes and five associated recoil proton scintillation counters positioned at the angles determined by the kinematics of the reaction. The general arrangement and data-acquisition logic were similar to that employed by Smith *et al.*[7] and Ottermann *et al.*[8] for various πd elastic scattering measurements at the Swiss Institute of Nuclear Research (SIN).

A. Pion beam

The pion beam emerging from the $M11$ channel was counted directly by the two coincident beam counters ($S1$ and $S2$) shown in Fig. 1. The active beam spot on target was determined by the dimensions of $S2$ (40 mm wide by 47 mm high) and by the convergence of the beam. The pion fraction of the beam was determined by particle time of flight through the channel and pulse height restrictions in $S2$ such as shown in Fig. 2. These data were recorded along with the $\pi^{\pm}$p data by means of a beam sampling trigger. The counters $S1$ and $S2$ were included in the event trigger (see caption to Fig. 1) so that any possible inefficiency in their response to pions did not affect the measured cross sections. A midchannel absorber reduced proton contamination in the positive pion beam. This absorber was also in place for the π^-p measurements.

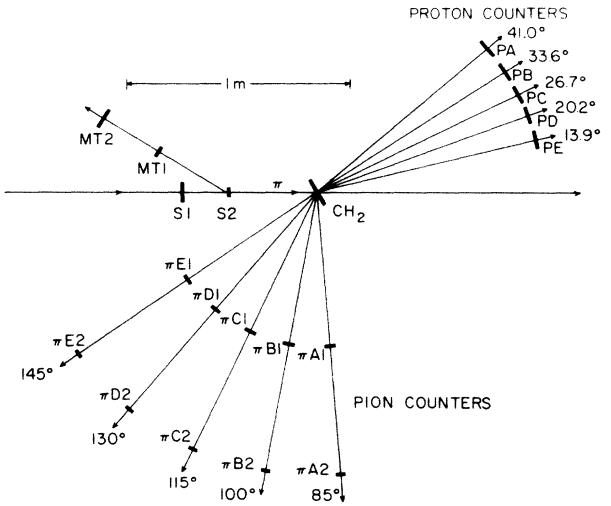

FIG. 1. Counter arrangement for coincidence measurements of πp elastic scattering at $T_\pi=90$ MeV. Five angles are measured simultaneously, and all particle flight paths are in air. A valid event for arm B, for example, is signaled by ($S1$)($S2$)($\pi B1$)($\pi B2$)(PB) and the proper TOF between $\pi B2$ and PB. Incident pion identification is given by rf-referenced TOF to $S2$ and the proper pulse amplitude in $S2$. MT1 and MT2 are monitor counters.

Remaining protons were eliminated with pulse height requirements on $S2$. To obtain the number of pions on target, corrections were made for pion decay over the distance starting upstream from $S2$ at the apex of the detected decay muon cone and extending to the target. A further small correction was made to account for two or more pions arriving at the target within one cyclotron rf cycle. The beam rates were typically 1×10^6 Hz, much smaller than the rf frequency (23×10^6 Hz), so these corrections to the cross section were of the order of 2%. A wire chamber two-dimensional beam profile monitor was inserted into the target position whenever the energy or the sign of the pion beam was changed in order to determine that the position and profile of the beam was satisfactory. This chamber was removed during data acquisition.

Major attention was devoted to accurate determination of the pion energy at the center of the scattering target. This is important because the differential cross sections in this energy region are steeply energy dependent, increasing at 2.5%—4.1% per MeV at $T_\pi=70$ MeV and 1.2%—2.2% per MeV at $T_\pi=140$ MeV for π^+, and at 1.3%—7.2% per MeV at $T_\pi=70$ MeV and 1.3%—2.5% per MeV at 140 MeV for π^-, depending on scattering angle.

The beam energy was determined by four methods. First,[9] the kinetic energy of the ions (d^+, t^+, $^3He^{2+}$, $^4He^{2+}$) from the pion production target was measured at the exit of the channel with a silicon surface-barrier detector. The surface-barrier detector was calibrated with an ^{241}Am α source. Second,[9] the time-of-flight difference for protons and pions was measured over the length of the channel. Third, the absolute time of flight was measured for pions over the distance from the pion production target to the $S1$ counter shown in Fig. 1. Fourth, the pion time of flight was measured between two counters, one at the channel exit and the other 4 m downstream. In the latter two methods, the electron component of the beam provided a velocity calibration. All four types of mea-

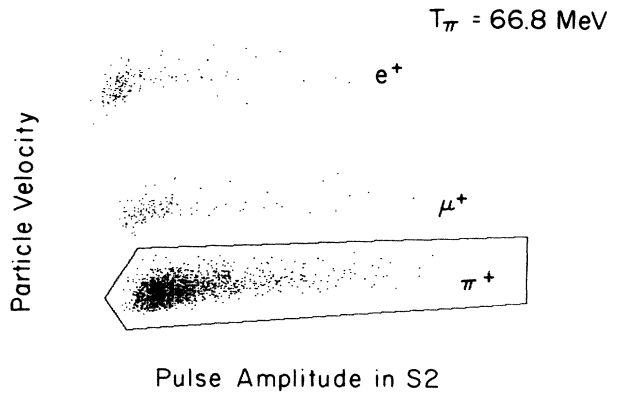

FIG. 2. A plot of particle velocity versus pulse amplitude in $S2$ for $T_\pi=66.8$ MeV. The particle velocity is determined by rf-referenced time of flight through the channel from the pion production target to $S2$. The box contains the pion component of the incident beam; above it are the muons, and above them the electrons.

surements were made at several channel momentum settings in the energy region of interest.

The conclusion formed by comparing the results of these measurements is that the central beam energies in the region of interest are known to ±0.5 MeV at the 95% confidence level. The full width momentum spread of the pion beam was typically $\Delta P/P=3\%$, corresponding to an energy spread of ±1.5 MeV at $T_\pi=67$ MeV and ±2.8 MeV at $T_\pi=139$ MeV. In practice, the central channel momentum is determined by NMR measurement of the fields in the channel dipoles. Pion energies at the channel exit are then corrected for absorption losses in the channel absorber, air, and scintillator elements between the channel exit and the target. A final correction, due to the target thickness and angle, is applied to give the pion energy at the target midplane.

B. Targets

Five different polyethylene targets were used in these measurements along with two graphite targets used for background determination. These targets are listed in Table I. The targets were all 12.7 cm×12.7 cm in area, and their thicknesses (in mg/cm^2) were determined by area and weight measurements. In addition, each target was checked for uniformity of thickness over its area. A commercial laboratory[10] provided an analysis of the hydrogen content of each target. The area, mass, and hydrogen content measurements were then combined to give the target densities in units of protons/cm^2 shown in Table I. The thicker targets were used primarily at the higher pion energies and for the larger pion scattering angles. The maximum useful target thickness was determined by proton energy loss and multiple scattering.

TABLE I. CH_2 targets used for data acquisition and carbon targets used for background determination. All targets were 12.7 cm×12.7 cm in area. The uncertainties shown in the third column are due to area and weight measurements. Those in the fourth column also include uncertainties in measured hydrogen content of the polyethylene (Ref. 10).

Target	Material	mg/cm^2	protons/cm^2 (×10^{21})
a	CH_2	44.0±0.1	3.78±0.04
b	CH_2	92.9±0.2	8.02±0.08
c	CH_2	156.9±0.2	13.5 ±0.1
d	CH_2	185.8±0.7	16.0 ±0.2
e	CH_2	294.2±0.3	25.3 ±0.3
C_1	graphite	199.5±0.1	
C_2	graphite	336.2±0.1	

C. Counters

The pion counters as shown in Fig. 1 were all passing plastic scintillators either 0.16 or 0.32 cm thick. All pion flight paths between the scintillators were in air.

The pion timing counters ($\pi 2$ in Fig. 1) defined the solid angles of the measurement; they were 4.00 cm wide by 10.00 cm high and were located at a radius of 130.0 cm from the target center. The first scattered pion counters ($\pi 1$ in Fig. 1) were sufficiently large (4.9 cm wide by 16.5 cm high) to cover the entire acceptance solid angle of the pion timing counters, and were at a radius of 72 cm from the target center. This telescope arrangement ensured that all analyzed events originated in the target.

The proton timing counters were also plastic scintillators. They were 9 cm wide by 40 cm high by 0.3 cm thick, with light guides and photomultipliers coupled at both the upper and lower ends. Timing information was derived from the sums of these two photomultiplier signals. The proton counters were sufficiently large to ensure that they did not limit the acceptance solid angles of the pion counter arms when operated in coincidence. They were at a radius of 100 cm.

A counter telescope arrangement was used to measure the efficiency of all the detectors. The result of this measurement was that for 19 of the 20 counters tested, the combined efficiency of the counter and coincidence circuitry was 1.000; for one counter it was 0.998. Consequently, no corrections to the data were necessary for counter or coincidence circuit inefficiency.

III. SYSTEMATIC TESTS

Extensive systematic tests were made to ensure that possible effects on the measured cross sections, such as deadtime, solid angles, multiple scattering, and decay corrections, were well understood. These tests fall into three classes: target thickness tests, beam rate tests, and geometry tests. The tests were done primarily with an 86.8 MeV π^+ beam, and cross sections measured under the differing conditions were compared. All of the cross sections were calculated using the appropriate Monte Carlo solid angles, which are discussed in more detail in Sec. IV. The counting statistics in these systematic tests were typically ±2%–4%.

The rate tests were performed at five beam rates between 0.5×10^6 π^+/s and 3.4×10^6 π^+/s, bracketing the data-taking range. Cross sections were measured at five angles between 77.5° and 145° (lab) at each rate. No statistically significant systematic trend of cross section with rate was evident.

Target thickness tests were done at four CH_2 target thicknesses between 44 and 387 mg/cm^2 at a beam rate of $(1.0\text{–}1.5)\times10^6$ π^+/s. Cross sections were measured at five angles between 77.5° and 145° (lab), except for the thickest target, where they were measured at four angles between 92.5° and 145° (lab). These target thickness tests were made with particular care because of concern about possible diminished πp coincidence efficiency due to proton energy loss and scattering in the target and nuclear reaction losses of pions and protons. If such a problem exists, it should be most evident for the smaller pion scattering angles and thicker targets. The results of these target thickness tests showed no statistically significant trend at any angle in measured cross section as the target thickness was varied. Our conclusion here is that coincidence inefficiency due to problems with proton escape from the target is less than 1%, even at 70 MeV.

A number of tests of sensitivity to experiment geometry were done. In the first set of tests, the angular locations

TABLE II. Center-of-mass differential cross sections. Uncertainties shown at each angle represent counting statistics and statistical uncertainties in the effective detector solid angles determined by the Monte Carlo process. Uncertainties in the absolute normalization (Δ) are shown separately at each energy. The pion energies have an uncertainty of ± 0.5 MeV.

π^+			π^-		
T_π(lab) (MeV)	$\theta_{\text{c.m.}}$ (deg)	$d\sigma/d\Omega$(c.m.) (mb/sr)	T_π(lab) (MeV)	$\theta_{\text{c.m.}}$ (deg)	$d\sigma/d\Omega$(c.m.) (mb/sr)
66.8	113.6	1.89±0.06	66.8	113.6	0.114±0.009
(Δ=1.2%)	127.5	2.43±0.07	(Δ=1.3%)	127.5	0.058±0.007
	138.5	2.78±0.09		138.5	0.065±0.008
	149.2	3.24±0.10		149.2	0.033±0.006
	159.7	3.49±0.09		159.7	0.032±0.006
86.8	89.6	1.94±0.04	86.8	89.6	0.253±0.011
(Δ=1.4%)	97.3	2.37±0.07	(Δ=1.2%)	104.7	0.191±0.010
	104.7	2.66±0.05		119.0	0.164±0.010
	112.0	3.19±0.09		132.5	0.143±0.010
	119.0	3.74±0.06		151.7	0.118±0.010
	125.9	4.15±0.11			
	132.5	4.73±0.07			
	139.1	5.16±0.13			
	151.7	6.20±0.08			
91.7	89.8	2.17±0.07	91.7	89.8	0.251±0.018
(Δ=1.2%)	104.9	3.10±0.09	(Δ=1.2%)	104.9	0.216±0.017
	119.2	4.26±0.12		119.2	0.176±0.017
	132.7	5.49±0.14		132.7	0.149±0.016
	151.8	7.03±0.17		151.8	0.156±0.018
97.9	90.1	2.46±0.06	97.9	90.1	0.301±0.009
(Δ=1.5%)	105.1	3.62±0.08	(Δ=1.2%)	105.1	0.221±0.008
	119.4	4.99±0.11		119.4	0.222±0.008
	132.9	6.59±0.13		132.9	0.230±0.009
	151.9	8.50±0.16		151.9	0.233±0.009
116.7	74.8	3.82±0.12	116.7	74.8	0.573±0.022
(Δ=2.3%)	85.6	3.98±0.13	(Δ=1.2%)	85.6	0.456±0.020
	90.8	4.17±0.11		90.8	0.421±0.019
	105.9	5.45±0.14		105.9	0.382±0.019
	113.0	6.89±0.21		113.0	0.409±0.022
	120.0	7.56±0.18		120.0	0.407±0.021
	133.4	10.10±0.23		133.4	0.485±0.024
	142.0	11.37±0.30		142.0	0.526±0.028
	152.3	13.76±0.28		152.3	0.608±0.029
	160.3	15.06±0.36		160.3	0.629±0.032
126.0	83.3	5.05±0.17	125.7	83.3	0.637±0.021
(Δ=2.5%)	91.2	5.38±0.16	(Δ=3.2%)	91.1	0.493±0.017
	98.8	5.69±0.20		98.8	0.494±0.019
	106.2	6.84±0.20		106.2	0.503±0.018
	113.4	7.77±0.25		113.4	0.488±0.020
	120.3	9.63±0.26		120.3	0.545±0.020
	127.1	10.86±0.32		127.1	0.643±0.025
	133.7	12.81±0.32		133.7	0.669±0.023
	140.1	14.25±0.39		140.1	0.779±0.028
	152.5	16.79±0.39		152.4	0.874±0.029
138.8	83.8	6.35±0.10	138.8	83.8	0.746±0.023
(Δ=2.3%)	91.6	6.26±0.12	(Δ=2.4%)	91.6	0.646±0.017
	99.3	7.40±0.12		99.3	0.614±0.022
	106.7	8.58±0.16		106.8	0.639±0.029
	113.8	10.25±0.17		113.8	0.671±0.025
	120.8	11.63±0.21		120.8	0.748±0.022
	127.5	13.54±0.22		127.5	0.924±0.031
	134.0	15.41±0.27		134.0	0.959±0.027
	140.4	17.52±0.27		140.4	1.106±0.036
	152.7	20.97±0.32		153.1	1.289±0.034

of the proton counters were varied from their kinematic centers. A proton counter displacement of ±1 degree from its kinematically defined angular location at $r=100$ cm had no discernible effect on the cross section. In a second test, increasing the target-to-proton-counter radius from 100 to 110 cm or from 100 to 130 cm produced no systematic change in the measured cross section. A third set of tests varied the pion counter geometry. Interchanging two pion telescopes or increasing the radius of a telescope by 19 cm had no discernible effect on the measured cross section. A fourth test used a beam spot of reduced area, obtained by rotating $S2$, the beam-definition scintillator, by 45° about a vertical axis. No statistically significant effect on the cross section was seen.

A summary of the systematic checks is given in Fig. 3. In this figure, the widths of the peaks (given by σ_x) are what one would expect from combining the individual measurements, each having 2–4% statistical precision, if no systematic effects are present. The statistical precision of centroid determination (given by $\sigma_{\bar{x}}$) is near 1%. The mean values (given by $\bar{x}$) in this figure are nonweighted averages and differ somewhat from our best cross section values given in Table II. This is because the tabulated cross sections are taken only from those measurements with optimum target thickness, beam rate, and detector geometry.

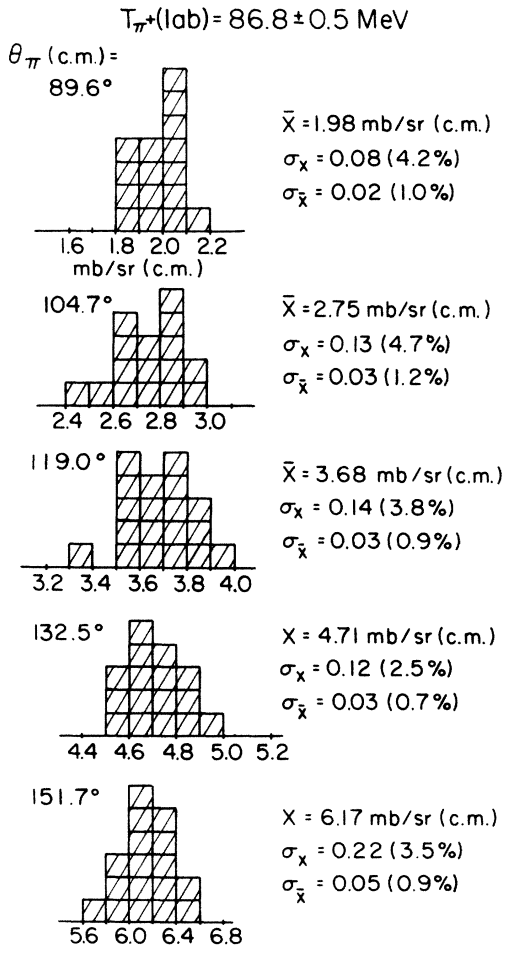

FIG. 3. Histograms of cross sections measured at 86.8 MeV to check systematic effects under varied experimental conditions. Included among the sixteen to nineteen points at each angle are measurements with CH_2 targets varying from 44 to 386 mg/cm^2, beam rates from 0.5 to 3.5 MHz, and various derangements of the counter geometry as discussed in the text. Also shown are the mean, standard deviation, and standard deviation of the mean for each histogram. (All cross section units are in mb/sr in the center-of-mass system.)

IV. ANALYSIS AND RESULTS

A. Cross section calculations

Differential cross sections at each scattering angle were calculated from the expression

$$\frac{d\sigma}{d\Omega}=\frac{Y\cos\theta_t}{\Delta\Omega(N_0)(\mathrm{LT})(\mathrm{beam}\times C_d\times F_\pi\times D)},$$

where Y is the number of counts recorded at that angle, θ_t is the target angle, $\Delta\Omega$ the effective counter solid angle (including decay of scattered pions) determined by Monte Carlo computation, N_0 the number of protons per square centimeter in the target, LT the data acquisition live time fraction, beam is the $S1$-$S2$ beam count, C_d is the correction for multiple pions in one beam burst, F_π is the pion fraction of the beam, and D is pion survival fraction from the $S1$-$S2$ beam definition telescope to the target. Cross sections computed from the above formula were increased by an energy-dependent factor, ranging from 0.7% to 0.9%, to account for nuclear reaction losses of pions and protons in the counters, counter light-shields, target, and air.

B. Background subtraction

Yields were determined from spectra of the time-of-flight (TOF) difference between the scattered pion and proton as shown in Fig. 4. No corrections to these spectra were made for randoms, which were never found to be

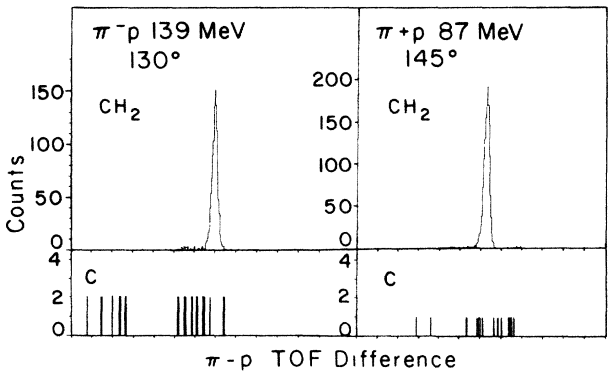

FIG. 4. The time-of-flight difference for one πp counter pair, shown for two cases at the indicated incident pion energy and scattering angle. The upper figures display the raw data, with no carbon or randoms subtraction. The lower figures show carbon spectra used for background subtraction. The full width at half maximum of each peak is about 400 ps.

more than 0.1% of the true coincidence rate.

Background runs were made at all beam energies for π^+ and at six beam energies for π^- with natural carbon targets either 200 or 336 mg/cm^2 thick. This was done to allow subtraction of events from the $^{12}C(\pi,\pi p)$ reaction from the πp TOF spectra as shown in Fig. 4. In general, the carbon subtraction was small, about 1% of the events, with some variation with angle and beam energy.

C. Beam scaling

Incident beam particles were counted as an $S1$-$S2$ coincidence, but the pion fraction and the number of pions per rf burst are also needed to determine the number of incident pions. The pion fraction was determined by plots such as Fig. 2, which display the pulse amplitude in $S2$ versus the rf-referenced particle time of flight through the channel. The pion fraction was determined run by run by use of box cuts as shown in the figure. This pion fraction is energy dependent, and ranged from 0.47 to 0.88 for π^- and from 0.83 to 0.97 for π^+. The fraction was determined to better than 1% at the low energies, but only to about 2% at 139 MeV, where the TOF separation is not as good.

The correction for multiple pions in one beam burst was also calculated run by run. A TOF-gated spectrum of the pion energy deposited in $S2$ reveals separate peaks for single and multiple pions. These peaks were fitted with a peak shape derived from a low-rate measurement and their areas determined. The resulting doubles-to-singles fraction (D/S) was checked by comparison to a rate-dependent curve generated from Poisson statistics. The two methods were found to be consistent and the rate-dependent D/S ratio was typically 1–3% at the beam rates used for data acquisition with an uncertainty as high as 15% of the D/S ratio. For cross section calculations, however, the doubles correction factor

$$C_d = \left[\frac{1+2D/S}{1+D/S} \right]$$

and the uncertainty in this quantity is typically only 0.4%.

D. Monte Carlo computations

In measurements of this type the effective solid angles of the coincident counter arrangement are modified from their simple geometrical values by a combination of effects which include beam convergence and size, Coulomb multiple scattering in the target and counter telescopes, and pion decays leading to muons which may not be detected in the telescopes. A Monte Carlo simulation of this arrangement has been used to study these effects separately and in combination to give an effective pion counter solid angle for use in cross section calculations.

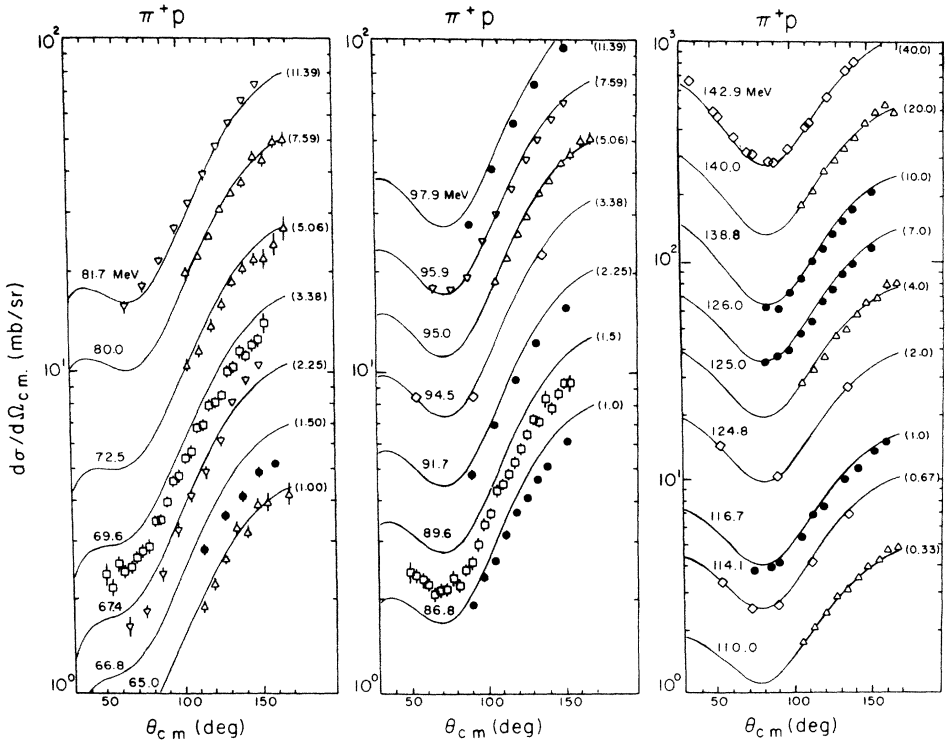

FIG. 5. Comparison of π^+p elastic differential cross sections measured in the present work with those obtained by four other groups. The solid lines are the phase-shift predictions from SAID SP86 (Ref. 12) at the indicated laboratory energies (above each curve), which correspond to each set of experimental data. The experimental cross sections and curves have been multiplied by the number given in parentheses at the right of each data set and curve. Cross sections from the present work are shown as solid dots (●). The other data are from Bussey *et al.* (Ref. 1) (◇), Bertin *et al.* (Ref. 2) (▽), Ritchie *et al.* (Ref. 3) (△), and Frank *et al.* (Ref. 4) (□).

In the Monte Carlo simulations, pions are assumed to be scattered uniformly in the center-of-mass frame (a reasonable assumption over the relatively small acceptance of the counter telescopes). Both pions and coincident protons are then tracked in the lab frame, where they Coulomb multiple scatter through each telescope element (target, air, scintillator, etc.) with scattering angle chosen from a Gaussian distribution with mean angular width inversely proportional to the product of momentum times velocity.[11] As pions are tracked through each element, the mean decay probability is calculated for that element. A decay in that element is simulated if a random number, greater than the above survival probability, is generated. If a decay occurs, the decay muon is tracked to see if it is indeed lost from the system.

The validity of the Monte Carlo simulation was thoroughly tested with a variety of experimental checks including data measured with several target thicknesses and deliberate shifts of the proton arms from their coincident angles. At 86.8 MeV, where the majority of the Monte Carlo tests were made, and with a 93 mg/cm^2 CH_2 target, Coulomb scattering corrections were typically 2%. In this case between 15% and 18% of the scattered pions decay, but when the decay muons are tracked the net decay correction is 11—14%. The solid angles determined by these Monte Carlo calculations typically differ from those determined by purely geometric calculations which include pion decay by 2—5%. All Monte Carlo calculations were run with a statistical precision of 1% in the effective solid angle.

E. Summary of experimental uncertainties

In addition to the counting statistics associated with each data point, there is also a ±1% statistical error due to the Monte Carlo process. These are the two components of the listed statistical error.

For a representative case, the normalization uncertainty includes errors due to multiple pions in one beam burst (0.4%), pion fraction of beam (1.5%), target thickness (1%), live time (0.2%), target angle (0.3%), pion decay (0.3%), counter geometry (0.2%), nuclear reaction losses of pions and protons (0.2%), carbon subtraction (0.1%), and randoms (0.0%). This would give a normalization uncertainty of ±1.9% in the absolute cross section.

F. Cross sections

The differential cross sections for πp elastic scattering measured in this work are listed in Table II. The uncertainties listed at each angle are the quadrature sums of counting statistics and the statistics of the Monte Carlo process. These statistical errors in the cross section range from less than 2% at several π^+ angles and energies to nearly 20% for π^- at 66.8 MeV. The larger values of these statistical errors are dominated by counting statistics. The normalization errors shown separately at each energy are dominated by the uncertainty in the pion fraction of the incident beam and the 1% uncertainty in target thickness.

Figures 5 and 6 show the cross sections from the present work as solid dots compared to several other published data sets. The curves are from the SAID SP86 phase-shift calculations of Arndt and Roper[12] for the indicated energies. These curves are included to facilitate comparison of cross sections measured at different energies and angles. The SP86 phase-shift calculations are constrained in magnitude by the πp elastic data of Refs. 1—3, in addition to other reaction data, but the data of Frank *et al.*[4] have had their normalization floated in SP86. The error bars shown in these graphs are statistical only; normalization errors are not included.

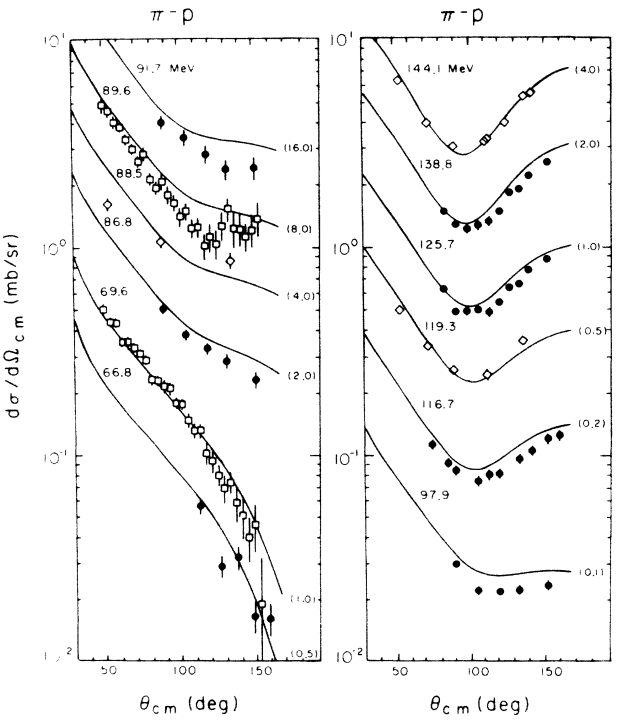

FIG. 6. Comparison of π^-p elastic differential cross sections measured in the present work with those obtained by two other groups. The solid lines are the phase-shift predictions from SAID SP86 (Ref. 12) at the indicated laboratory energies (above each curve), which correspond to each set of experimental data. The experimental cross sections and curves have been multiplied by the number given in parentheses at the right of each data set and curve. Cross sections from the present work are shown as solid dots (●). The other data are from Bussey *et al.* (Ref. 1) (◇) and Frank *et al.* (Ref. 4) (□).

V. DISCUSSION AND CONCLUSIONS

The present π^+p data shown in Fig. 5 all lie beneath the SP86 phase-shift curves, but the difference between data and prediction is vanishingly small at the higher energies. At the lower energies, the discrepancy increases but tends to be less for the smaller pion scattering angles (and smaller scattered proton energies), suggesting that the discrepancy cannot be an experimental problem related to proton scattering and energy loss in exiting from the target.

At 126.0 and 138.8 MeV, the present π^+p data very

nearly correspond to the phase shifts which fit the data of Ritchie *et al.*[3] at 140.0 MeV and Bussey *et al.*[1] at 142.9 MeV. At 66.8, 86.8, and 91.7 MeV the present measurements lie well below the values computed by SAID SP86 from the results of Bertin *et al.*,[2] Bussey *et al.*,[1] and Ritchie *et al.*,[3] but do seem to be entirely consistent with the recent data of Frank *et al.*[4] at 69.6 and 89.6 MeV for pion scattering angles larger than 100°. However, the present data at 86.8 and 66.8 MeV tend toward better agreement with SP86 as one goes to smaller scattering angles. This is in contrast to the data of Ref. 4 at 89.6 and 69.6 MeV, which depart increasingly from SP86 at the smaller scattering angles. Thus the differences between the present work and that of Ref. 4 cannot be ascribed entirely to a normalization problem.

The present π^-p data follow the pattern of the π^+p data in that they generally lie below the SP86 phase shift curves. At our lowest three energies, the cross sections are generally consistent with the data of Frank *et al.*[4] at 69.6 and 89.6 MeV, and at our highest three energies the present data lie below values computed by SAID SP86 from the measurements of Bussey *et al.*[1]

ACKNOWLEDGMENTS

We thank T. Cunningham for his assistance in data acquisition and analysis, and D. Vanderweit for his help in data analysis. This work was supported in part by the Natural Sciences and Engineering Research Council of Canada, the U.S. Department of Energy, and by a NATO fellowship for one of the authors (R.P.T.) via the Deutscher Akademischer Austauschdienst (DAAD).

[1] P. J. Bussey *et al.*, Nucl. Phys. **B58**, 363 (1973).
[2] P. Y. Bertin *et al.*, Nucl. Phys. **B106**, 341 (1976).
[3] B. G. Ritchie *et al.*, Phys. Lett. **125B**, 128 (1983).
[4] J. S. Frank *et al.*, Phys. Rev. D **28** 1569 (1983).
[5] M. E. Sadler, First Workshop on Pion-Nucleon Scattering, Karlsruhe, West Germany, Aug. 1983 (unpublished).
[6] P. B. Siegel and W. R. Gibbs, Phys. Rev. C **33**, 1407 (1986).
[7] G. R. Smith *et al.*, Phys. Rev. C **29**, 2206 (1984).
[8] C. R. Otterman *et al.*, Phys. Rev. C **32**, 928 (1985).
[9] These two measurements were performed by C. Oram and D. Ottewell and are described in a TRIUMF internal report and in the 1985 TRIUMF Progress Report.
[10] Galbraith Laboratories, Knoxville, TN.
[11] C. G. Wohl *et al.*, Rev. Mod. Phys. **56**, S1 (1984).
[12] R. A. Arndt and L. O. Roper, SAID on-line program.